



“I do not feel my hand where I see it”: causal mapping of visuo-proprioceptive integration network in a surgical glioma patient

Emmanuel Mandonnet^{1,2,3} · Daniel Margulies³ · Chloe Stengel³ · Mélissa Dali¹ · François Rheault⁴ · Monica N. Toba^{3,5} · François Bonnetblanc⁶ · Antoni Valero-Cabre³

Received: 31 March 2020 / Accepted: 6 May 2020 / Published online: 13 May 2020
© Springer-Verlag GmbH Austria, part of Springer Nature 2020

Abstract

A recent tasked-based fMRI study unveiled a network of areas implicated in the process of visuo-proprioceptive integration of the right hand. In this study, we report a case of a patient operated on in awake conditions for a glioblastoma of the left superior parietal lobule. When stimulating a white matter site in the anterior wall of the cavity, the patient spontaneously reported a discrepancy between the visual and proprioceptive perceptions of her right hand. Using several multimodal approaches (axono-cortical evoked potentials, tractography, resting-state functional connectivity), we demonstrated converging support for the hypothesis that tumor-induced plasticity redistributed the left-lateralized network of right-hand visuo-proprioceptive integration towards its right-lateralized homolog.

Keywords Visuo-proprioceptive integration · Awake surgery · Functional connectivity · Structural connectivity

Introduction

Our brain is able to build an internal representation of our body parts by linking the afferent information coming from the sensory modalities of vision, proprioception, and touch.

This article is part of the Topical Collection on *Functional Neurosurgery - Other*

✉ Emmanuel Mandonnet
mandonnet@mac.com

¹ Department of Neurosurgery, Lariboisière Hospital, APHP, 2 rue Ambroise Paré, 75010 Paris, France

² University Paris 7, Paris, France

³ Frontlab, ICM, Paris, France

⁴ Sherbrook connectivity imaging lab, department of computer science, Faculty of sciences, Université de Sherbrooke, Sherbrooke, Canada

⁵ Laboratory of Functional Neurosciences (EA 4559), University Hospital of Amiens and University of Picardy Jules Verne, Amiens, France

⁶ INRIA, University of Montpellier, LIRMM, CAMIN team, Montpellier, France

While visual information has long been thought to prevail over proprioceptive information in this process, psychological experiments have demonstrated that the weight of the actual contribution of vision and proprioception in estimating an integrated hand position varied with the direction [17]. For example, the estimate of hand position in the depth direction is more informed by proprioceptive than visual information [17].

More recently, an fMRI study unveiled a network showing higher activity levels when visual and proprioceptive information about a subject's right-hand position was congruent rather than incongruent [8]. More specifically, the identified system encompassed several left-lateralized areas, including the anterior and posterior superior parietal lobule, the extrastriate body area (EBA) [5], the inferior parietal lobe, and the ventral premotor cortex. Importantly, all these areas increased their functional connectivity with visual V1 areas in the congruent versus incongruent condition.

In the present study, we report the case of a patient operated on in the awake condition for a glioblastoma of the left superior parietal lobule. We found an anterior site in the wall of the resection whose stimulation induced in the patient a conscious feeling that there was a discrepancy between the visual and proprioceptive perceptions of her right hand. We posited that

this site was an input gate into the network of visuo-proprioceptive integration [10] and sought to describe this network further by combining different methodologies (axono-cortical evoked potentials, tractography, and resting-state functional connectivity). Finally, by comparing its topography with the one found in healthy individuals [8], we put forward the hypothesis that tumor-induced plasticity redistributed the left-lateralized network towards its right-lateralized homolog.

Methodology

Ethics statement

Patient gave full informed consent to participate to this study, which was approved by the ethics committee of Saint-Louis hospital (reference 2013/51).

Patient-case

A 62-year-old woman, right-handed, was admitted in our department after acute onset episodes of visual troubles in the right hemifield. She was working as an administrative manager in a petrochemical company. MRI revealed a contrast-enhanced left superior parietal lobule lesion (see Fig. 1). Surgery in the awake condition was offered, in order to resect a marginal zone around the contrast-enhanced area while minimizing functional risk. Tumor resection was complete, and the patient was discharged at post-operative day 3. Pathological analysis confirmed the diagnosis of glioblastoma.

Cortical and axonal mapping in awake patient

Surgical resection was functionally guided, by making use of brain mapping with electrical stimulation, as previously described [2, 9, 11]. Direct electrical stimulation at 60 Hz was applied to the cortical surface or white matter, while the patient performed tasks assisted by a speech therapist. The impact of stimulation was feedbacked to the surgeon by the therapist in charge of observing and documenting the patient's behavior (such as the arrest of ongoing movements, unexpected feelings). Electrical stimulation was delivered with human use certified intraoperative equipment (Nimbus i-Care light, Innopsys, Narbonne, France) delivering constant-current biphasic square pulses (single pulse duration of 500 μ s, total duration of 1000 μ s) with a bipolar stimulation probe (two straight 1.5 mm diameter electrode tips with a pitch of 5 mm, forming a “Y”), kept in direct contact with white matter tissue typically for 3 s. Stimulus intensity was progressively increased by 0.5 mA steps starting from 1 mA, until eliciting observable changes in patient's behavior, and up to a maximum of 4 mA, in order to limit the risk of a seizure.

Axono-cortical evoked potentials recordings

Once tumor resection was achieved, a white matter site previously identified as functionally eloquent (when probed with bursts of electrical pulses at a frequency of 60 Hz) was stimulated this time at a frequency of 1 Hz (1 pulse per second). The stimulated white matter location was registered on the patient's preoperative MRI with a frameless neuronavigation system (S7, Medtronic, MN, USA). Stimulation intensity was set at 3 mA, the same intensity at which 60 Hz stimulation had induced a motor dysfunction during white matter mapping.

Fig. 1 Intraoperative photography. Upper left, cortical mapping. Tag 2, right arm tingling at 2.5 mA. Lower left, electrodes location. Upper right, final mapping. Tag 6, when stimulating at 3 mA, the patient said “I do not feel my (right) hand where I see it”. Lower right, neuronavigation snapshot locating tag 6 in the preoperative MRI

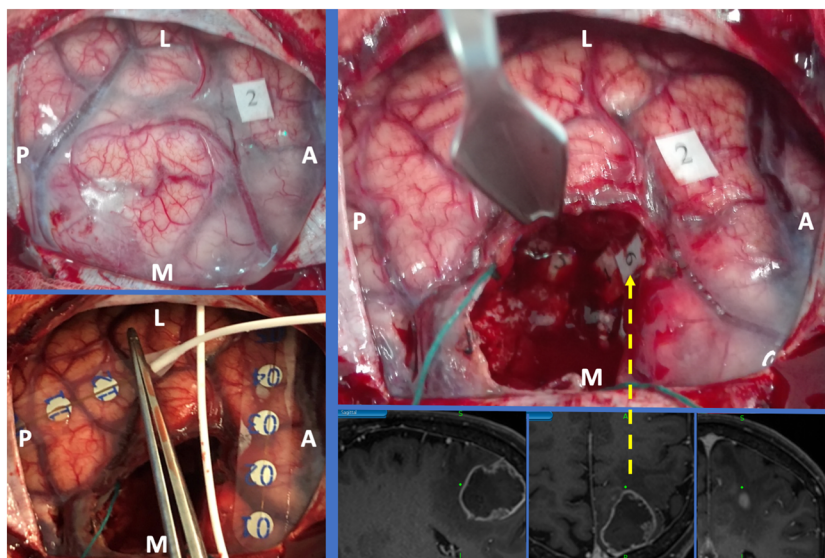
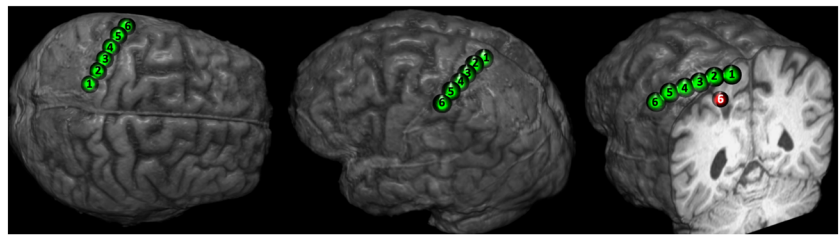


Fig. 2 Locating electrodes contact and tag 6 in the post-operative MRI. Only strip 1 contacts were represented, as no ACEPs were recorded on strip 2 contacts



Sets of 60 s recordings (~60 pulses at 1 Hz for 1 min) were obtained. In order to tease apart electrical stimulus artifacts from biological evoked neural signals, stimulation was repeated inverting the first polarity of the biphasic electrical pulse (500 μ s/phase, for a total biphasic pulse duration of 1000 μ s) [18].

Two electrode strips of 6×1 contacts each (Dixi medical, Chaudfontaine, France, radius 2.5 mm, inter-electrode distance 1 cm) were placed over the postcentral gyrus (contacts 1 to 6, from dorso-mesial to ventro-lateral) and the angular gyrus/lateral occipital cortex (contacts 7 to 12, from anterior to posterior), respectively (see Fig. 1).

Signals were recorded in a referential montage (i.e., with a reference electrode placed on the skin overlying the petrous portion of the left mastoid bone) for the postcentral gyrus strip and in differential montage for the other strip. A common ground electrode was placed on the skin of the right scapular bone. Cortical potentials were recorded using continuous electrocorticography (ISIS-IOM, Inomed GmbH, Emmendingen, Germany) acquired with the following parameters: sampling rate, 2000 Hz; amplitude coding, 16 bits; high-pass filter of 0.5 Hz; active 50 Hz notch filter.

Evoked-potentials analysis

Data were analyzed offline with a custom-made MATLAB script (written by MD) (MathWorks, Natick, MA, USA). For each individual evoked potential, pre-stimulus baseline was determined by averaging over 100 ms before the stimulus onset. This offset was then subtracted to each potential, thus normalizing each pre-stimulus potential to zero. Waveforms

elicited by the stimulus were time-locked to the electrical pulse onset and averaged through. The mean evoked potential was then filtered to remove the stimulation artifact (Butterworth low pass filter with stop band frequency of 100 Hz, and Stop band attenuation of 10 dB).

Imaging

Diffusion-weighted imaging (DWI) and resting-state fMRI (rs-fMRI) were acquired 4-months post-surgery. A 3T Siemens Skyra system (Siemens, Erlangen, Germany) with a 64-channel phased-array head coil was used to acquire DWI of the whole head with an anterior-posterior phase of acquisition. DWI parameters consisted in an acquisition matrix of $108 \times 108 \times 120$ voxels of 2.3 mm^3 with a total field of view of $250 \times 250 \times 120 \text{ mm}^3$. DWI was acquired along 64 directions with a weighting $b = 2000 \text{ s/mm}^2$. Additionally, non-weighted ($b = 0$) volumes were also acquired. Echo time (TE) was set at 95 msec and repetition time (TR) at 7700 msec. The whole sequence lasted 9:45 min. During the rs-fMRI scanning, the participant was instructed to rest, but to remain awake with his eyes closed. A gradient echo planar imaging (EPI) sequence was used to acquire 130 volumes ($94 \times 94 \times 36$ voxels, $2.1 \times 2.1 \times 3 \text{ mm}^3$, and a field of view of $200 \times 200 \times 108 \text{ mm}^3$). The TR was 3200 msec, and the TE was 30 msec. The total rs-fMRI scan duration was 7 min.

Tractography

Tractograms were obtained using a home-made pipeline. From the $b = 2000 \text{ mm}^2/\text{s}$ volumes, fiber orientation

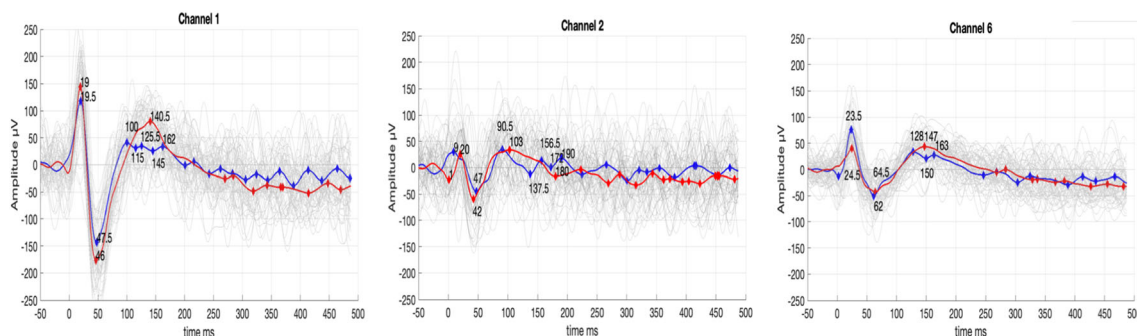


Fig. 3 ACEPs obtained on contacts 1, 2, and 6. Note that the amplitude corresponds to (reference–contact). The red and blue curves correspond to the two opposite polarity in the biphasic pulse (positive-negative versus negative-positive)

Table 1 Amplitudes and delays of the N1 and N2 troughs of ACEPs

	N1 delay (ms)	N1 amplitude (μ V)	N2 delay (ms)	N2 amplitude (μ V)
C1	19.6+–1.1	123.7+–15.4	122.5+–3.3	43.1+–7.3
C2	8.8+–3.3	31.1+–13.1	97.5+–3.9	35.9+–10.5
C3	∅	∅	∅	∅
C4	∅	∅	∅	∅
C5	∅	∅	∅	∅
C6	23.6+–1.1	80.1+–8.6	138.8+–3.5	35.9+–6.1

distribution function (fODF) was estimated using constrained spherical deconvolution (CSD) [3, 15]. Probabilistic tractography [4, 16] was subsequently computed with 10^5 initial seeds. Seeding and tracking masks were obtained by thresholding the FA map at 0.10. Tractograms were dissected with MI-Brain software.

Resting-state functional connectivity analysis

Resting-state sequences were processed with the AFNI pipeline `uber_subject.py`, with default settings, except censor motion limit, which was set at 0.8 mm instead of the more stringent value of 0.2 mm. This value was the minimal value without censoring any time points. A 5 mm radius spheric ROI was placed on the location of electrode contact 1 and served as a seed region for functional connectivity analysis (function `3dUndump` and `3dmaskave`). The whole-brain correlation map (function `3dfim+`) was upsampled to the 1 mm resolution of the T1 anatomical image. The anatomical T1 sequence was co-registered to the MNI space using ANTS, and the transformation was applied to the 1 mm resolution correlation map. This map was then thresholded (using `3dclust`, with `-1clip` option set at 0.47 and `-NN2` option set at 40) and finally visualized using MRIcron software.

Table 2 Amplitudes and delays of the N1 and N2 troughs of reverse polarity

	N1 delay (ms)	N1 amplitude (μ V)	N2 delay (ms)	N2 amplitude (μ V)
C1	19.0+–0.0	151.6+–8.9	122.5+–1.7	85.8+–5.5
C2	20.0+–0.0	27.3+–6.2	97.5+–7.5	36.6+–8.3
C3	∅	∅	∅	∅
C4	∅	∅	∅	∅
C5	∅	∅	∅	∅
C6	24.5+–0.5	42.0+–5.0	138.8+–3.8	45.7+–5.0

Table 3 Count of streamlines joining the tag 6 to the different contacts

	Tag 6	Tag 6 and thalamus	Tag 6 and corpus callosum
C1	121	8	74
C2	113	21	36
C3	2	0	1
C4	2	0	0
C5	0	0	0
C6	0	0	0

Among these streamlines, the numbers of those passing through the corpus callosum or ending in the thalamus are also given

Results

Mapping

Cortical mapping revealed a site (tag 2) whose stimulation at an intensity of 2.5 mA generated tingling in the right arm. At the end of the resection, several functionally eloquent sites were identified in the white matter: dorso-mesially (tag 3, not visible on the intraoperative photography) a site generating feeling of vibration in the right leg when stimulated at an intensity of 3 mA; these fibers were detected also more ventrally (tag 4). Just latero-dorsally to the latter, another white matter site generated a discrepancy between visually and proprioceptively perception of the right hand (the patient spontaneously reported during stimulation “I do not feel my hand where I see it”) when stimulated at an intensity of 3 mA

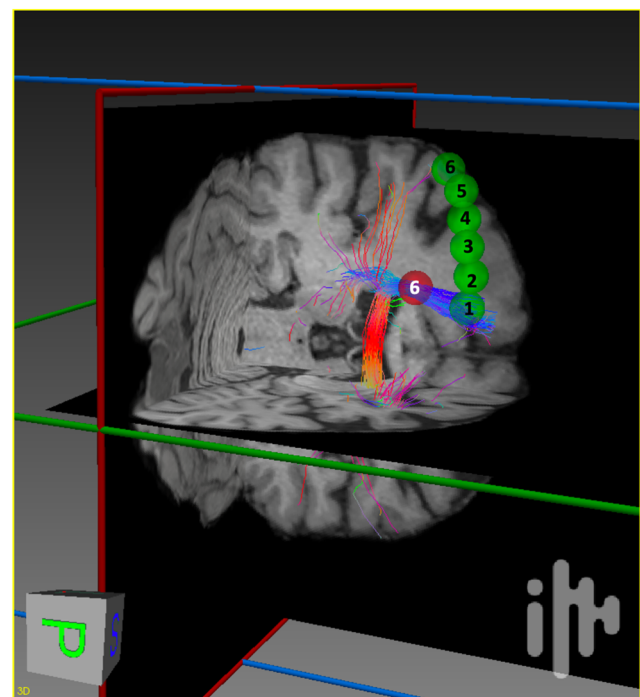
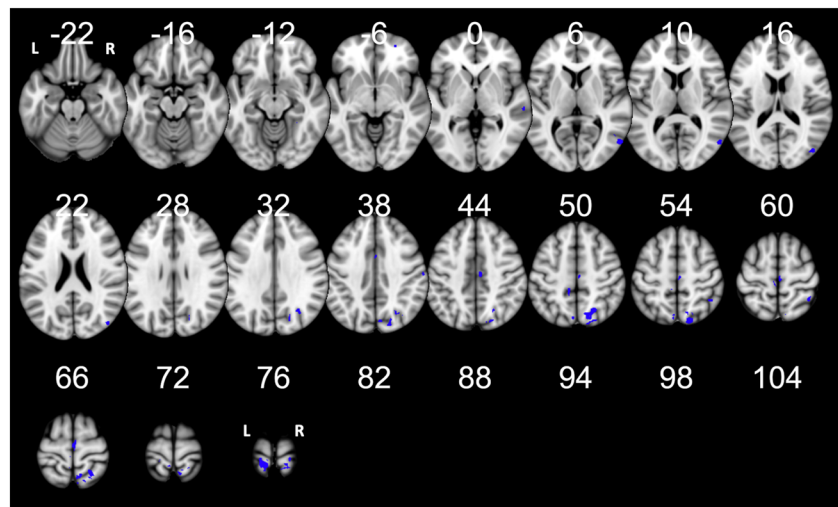
**Fig. 4** 3D view of streamlines joining tag 6 and contact 1

Fig. 5 rs-fMRI functional connectivity of contact 1. Note that, apart from the cluster surrounding the seed region, all clusters are located in the right hemisphere



(see Fig. 1, tag 6). Finally, the stimulation of tag 5 at 5 mA induced a vertigo.

Axono-cortical evoked potentials

Strip 1 (referential montage: reference minus contact) was positioned all over the most rostral portion of the superior parietal lobule and post-central gyrus (see Figs. 1 and 2). Strip 2 (differential montage between adjacent contacts) was located over the angular and lateral occipital cortex (see Fig. 1). When stimulating tag 6, the larger ACEP was recorded on contact 1 of strip 1 (see Fig. 3 and Tables 1 and 2). A smaller ACEP was recorded on contact 2, with the very same shape of contact 1. Finally, an even smaller ACEP was recorded on contact 6. No ACEPs were recorded by contacts 3, 4, and 5 in strip 1 or by any contacts in strip 2.

Tractography

A 1 cm-diameter spherical ROI corresponding to tag 6 was manually positioned on the postoperative T1 anatomical image (see Fig. 2), based on the neuronavigation snapshot and

intraoperative photography (see Fig. 1). This ROI defined a seed for dissecting the postoperative tractogram. The electrode contacts were also positioned on the postoperative T1 anatomical image, following the methodology described in [2].

The tractogram comprised a total of 70,825 streamlines. Table 3 gives the number of streamlines joining the stimulation site to each contact. Contacts 1 and 2 had the greatest number of connections to the stimulation site. Figure 4 shows the streamlines connecting the stimulation site tag 6 and contact 1. A majority of these streamlines either passed through the corpus callosum or terminated in the thalamus. Finally, after ANTS registration of the T1 anatomical postoperative image to the MNI template, the coordinates of the tag 6 ROI were obtained as $x = -22$, $y = -40$, and $z = 56$ and the coordinates of the contact 1 as $x = -16$, $y = -39$, and $z = 76$.

Resting-state functional connectivity

A 5 mm-radius spherical ROI was put at the location of contact 1. The maps showing the postoperative ROI-to-voxel connectivity is given in Figs. 5 and 6. Table 4 gives the MNI coordinates of the different clusters. Apart from the cluster

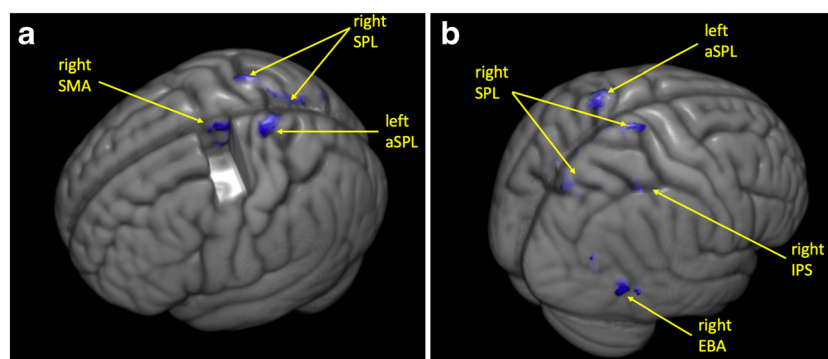


Fig. 6 rs-fMRI functional connectivity of contact 1. The seed ROI has been put just beneath contact 1, in the anterior superior parietal lobule. **a** Postero-superior view. A cut has been made within the left precentral

gyrus, in order to visualize the right SMA cluster. **b** Posterolateral view. SPL, superior parietal lobule; SMA, supplementary motor area; IPS, intraparietal sulcus; EBA, extrastriate body area

surrounding the seed ROI, all clusters were localized in the right hemisphere, including the right superior parietal lobule, the right supplementary motor area, and the right anterior middle occipital gyrus.

Discussion

In this study, we explored the network of visuo-proprioceptive integration of the right hand through an input gate that was determined by intraoperative behavioral impairment induced by 60 Hz electrical stimulation of a site within the white matter of the anterior left superior parietal lobule. By tractography and ACEPs, we located the cortical area linked to this input gate in the anterior left superior parietal lobule. Such a result is in good agreement with the claim that the superior parietal lobule is an essential node for storing the internal state estimate of our own body [19]. It is also in line with a previous study demonstrating, in the context of stereo-electroencephalography in patients explored for drug-resistant epilepsy, that electrical stimulation within the superior parietal lobule yielded visual illusions and/or body scheme alterations, although similar effects were also observed within the inferior parietal lobe and intraparietal sulcus [1]. We then used this area as a seed for mapping the network using resting-

state functional connectivity analysis. By doing so, we found a right-lateralized network, comprising clusters in the right superior lobule, right EBA, and right supplementary motor area. This network is consistent with a mirrored version of the left-lateralized network unveiled in Limanowski et al. [8]. It is thus tempting to put forward the hypothesis that tumor-induced plasticity redistributed the healthy subject left-lateralized network towards its right-lateralized homolog. Note that the preservation of callosal fibers (see Fig. 4 and Table 3) is of utmost importance in order to keep the link between the node in the left anterior superior parietal lobule and the redistributed right-lateralized areas.

One may ask why the cortical mapping did not demonstrate a site generating the same disruption of visuo-proprioceptive integration. One hypothesis could be that the stimulated area was too restricted and that the effect would have been obtained only by a higher stimulus intensity or a multisite stimulation [6], thus disrupting a region that would comprise both contacts 1 and 2.

Finally, this study fully supports the necessity to wake patients when operating on tumors in the superior parietal regions in order to map body scheme [14]. Detecting deficits of body scheme representations requires a thorough neuropsychological assessment, in order to go beyond the classical signs of parietal syndromes, as reported by neurological examination in previous surgical series of parietal lobe tumors

Table 4 MNI coordinates of the rs-fMRI functional connectivity clusters from a seed located in contact 1

<i>X</i>	<i>Y</i>	<i>Z</i>	Number of voxels	Homolog regions of Limanowski et al.
19.00	− 76.00	44.00	1630	pSPL
2.00	− 15.00	66.00	598	
− 12.00	− 42.00	77.00	527	
18.00	− 38.00	79.00	514	
56.00	− 67.00	6.00	507	EBA
44.00	− 78.00	18.00	266	
22.00	− 51.00	67.00	221	aSPL
43.00	− 49.00	56.00	167	
− 9.00	− 38.00	51.00	124	
1.00	2.00	35.00	105	
− 4.00	− 73.00	49.00	95	
− 3.00	− 30.00	63.00	71	
41.00	14.00	1.00	62	
61.00	− 16.00	37.00	58	SMG
26.00	54.00	− 4.00	56	
7.00	− 76.00	36.00	55	
62.00	− 23.00	1.00	43	
31.00	− 44.00	− 9.00	41	
60.00	− 60.00	4.00	40	
16.00	− 62.00	64.00	40	

Note that out of 20 clusters, only 4 are left-lateralized. The last column gives the labelling given in Limanowski et al. of some anatomical clusters after a left-right flip

[12, 13]. To this regard, the present study is in line with the series of Herbet et al. [7], reporting that patients with tumor resections located in the anterior superior parietal lobule experienced more frequently troubles of body awareness. In particular, by using network lesion-symptom mapping, they also characterized a network consistent with that found by Limanowski et al. [8].

Conclusion

In this case report, we provide a causal evidence for the role of the left anterior superior parietal lobule in the visuo-proprioceptive integration of the right hand. By means of multimodal mapping, we suggest that this area is an essential node of a visuo-proprioceptive integration network identified previously [7, 8, 19]. Moreover, our case provides a basis to hypothesize that, in presence of a lesion of the left superior parietal lobule, the left-lateralized network normally connected to this node can be redistributed to its contralateral homolog, owing to reshaping through mechanisms of plasticity. This hypothesis awaits further confirmation from a larger series of cases.

Funding information MD was supported by the CRC-chirurgie 2016 from AP-HP. EM was supported by INSERM, contract interface 2018.

Compliance with ethical standards

Patient gave full informed consent to participate to this study, which was approved by the ethics committee of Saint-Louis hospital (reference 2013/51).

Patient consent The patient has consented to the submission of the case report for submission to the journal. This case report has been written in accordance with COPE guidelines and comply with the CARE statement.

References

- Balestrini S, Francione S, Mai R, Castana L, Casaceli G, Marino D, Provinciali L, Cardinale F, Tassi L (2015) Multimodal responses induced by cortical stimulation of the parietal lobe: a stereo-electroencephalography study. *Brain* 138(Pt 9):2596–2607
- Corrivetti F, de Schotten MT, Poisson I, Froelich S, Descoteaux M, Rheault F, Mandonnet E (2019) Dissociating motor-speech from lexico-semantic systems in the left frontal lobe: insight from a series of 17 awake intraoperative mappings in glioma patients. *Brain Struct Funct* 224(3):1151–1165
- Descoteaux M, Angelino E, Fitzgibbons S, Deriche R (2007) Regularized, fast, and robust analytical Q-ball imaging. *Magn Reson Med* 58(3):497–510
- Descoteaux M, Deriche R, Knösche TR, Anwander A (2009) Deterministic and probabilistic tractography based on complex fibre orientation distributions. *IEEE Trans Med Imaging* 28(2):269–286
- Downing PE, Jiang Y, Shuman M, Kanwisher N (2001) A cortical area selective for visual processing of the human body. *Science* 293(5539):2470–2473
- Gonen T, Gazit T, Korn A, Kirschner A, Perry D, Hendler T, Ram Z (2017) Intra-operative multi-site stimulation: expanding methodology for cortical brain mapping of language functions. *PLoS One*. <https://doi.org/10.1371/journal.pone.0180740>
- Herbet G, Lemaitre A-L, Moritz-Gasser S, Cocheureau J, Duffau H (2019) The antero-dorsal precuneal cortex supports specific aspects of bodily awareness. *Brain* 142(8):2207–2214
- Limanowski J, Blankenburg F (2016) Integration of visual and proprioceptive limb position information in human posterior parietal, premotor, and extrastriate cortex. *J Neurosci* 36(9):2582–2589
- Mandonnet E (2019) Transopercular resection of IDH-mutated insular glioma: a critical appraisal of an initial experience. *World Neurosurg*. <https://doi.org/10.1016/j.wneu.2019.08.071>
- Mandonnet E, Winkler PA, Duffau H (2010) Direct electrical stimulation as an input gate into brain functional networks: principles, advantages and limitations. *Acta Neurochir* 152(2):185–193
- Mandonnet E, De Witt HP, Poisson I et al (2015) Initial experience using awake surgery for glioma: oncological, functional, and employment outcomes in a consecutive series of 25 cases. *Neurosurgery* 76(4):382–389 discussion 389
- Russell SM, Elliott R, Forshaw D, Kelly PJ, Golfinos JG (2005) Resection of parietal lobe gliomas: incidence and evolution of neurological deficits in 28 consecutive patients correlated to the location and morphological characteristics of the tumor. *J Neurosurg* 103(6):1010–1017
- Sanai N, Martino J, Berger MS (2012) Morbidity profile following aggressive resection of parietal lobe gliomas. *J Neurosurg* 116(6):1182–1186
- Schwoebel J, Coslett HB (2005) Evidence for multiple, distinct representations of the human body. *J Cogn Neurosci* 17(4):543–553
- Tournier J-D, Calamante F, Connelly A (2007) Robust determination of the fibre orientation distribution in diffusion MRI: non-negativity constrained super-resolved spherical deconvolution. *Neuroimage* 35(4):1459–1472
- Tournier J-D, Calamante F, Connelly A (2012) MRtrix: diffusion tractography in crossing fiber regions. *Int J Imaging Syst Technol* 22(1):53–66
- Van Beers RJ, Wolpert DM, Haggard P (2002) When feeling is more important than seeing in sensorimotor adaptation. *Curr Biol* 12(10):834–837
- Vincent M, Guiraud D, Duffau H, Mandonnet E, Bonnetblanc F (2017) Electrophysiological brain mapping: basics of recording evoked potentials induced by electrical stimulation and its physiological spreading in the human brain. *Clin Neurophysiol* 128(10):1886–1890
- Wolpert DM, Goodbody SJ, Husain M (1998) Maintaining internal representations: the role of the human superior parietal lobe. *Nat Neurosci* 1(6):529–533

Publisher's note Springer Nature remains neutral with regard to jurisdictional claims in published maps and institutional affiliations.